On the relation between battery size and PV power ramp rate limitation

Aitor Makibar , Luis Narvarte, Eduardo Lorenzo

A B S T R A C T

PV power fluctuations caused by clouds are leading operators of grids with high renewable energy penetration rates to impose ramp rate limitations. Costly battery energy storage systems are used for fulfilling these regulations but the question of the power and energy requirements for accomplishing them has not been fully answered. This work analyses the effects of reducing the size of a battery designed to absorb every fluctuation by taking into consideration, both, the fluctuation occurrence and the penalties in case of non-compliance of a given prescribed ramp-rate limitation. A theoretical analysis was carried out in order to assess the relation between size reduction and ramp rate compliance, obtaining as result a model for predicting the probability of non-compliances with a reduced battery. Additionally, the battery size reduction analysis was applied to the particular grid code currently proposed for Puerto Rico, creating new tools for selecting a battery with reduced power and energy capacity.

1. Introduction

Cloud passing over PV generators translates into short-term – seconds or few minutes – PV power fluctuations, which represent troubles for maintaining the frequency and voltage stability in electric grids including PV plants (Marcos et al., 2011a). This issue becomes particularly relevant in relatively small grids, such as islands or scarcely interconnected regions, because smoothing effects derived from the aggregation of geographical dispersion are intrinsically limited (Lave et al., 2012; Marcos et al., 2012). Not surprisingly, a growing number of such small grid regulations are imposing ramp-rate limits to the power injected by PV plants at the point of common coupling (PCC). The door for such limitations has been opened in PREPA, 2012 by the Puerto Rico Electric Power Authority, PREPA, by imposing a 10% of plant nameplate PV power per minute ramp rate limitation, RR_{LIM} = 10% per minute. Other TSOs are also concerned about this matter, with even more restrictive ramp rates (CRE, 2012; HECO, 2014; NERC, 2012).

Accomplishing such regulations requires a battery energy storage system (BESS), able to inject (absorb) power when the PV power decreases (increases) faster than the prescribed limit. Fig. 1a shows the configuration of a PV plant supported by a BESS on its PCC. In such a configuration, the result is a ramp shaped injection to the grid for highly fluctuating periods. Fig. 1b shows for a period of around 30 min the output power of a multi-MW PV plant, $P_{PV}(t)$, and the power injected to the grid, $P_{GRID}(t)$, applying ramp rate control by means of the BESS. It can be seen that when a cloud front passes over the plant, the PV power falls suddenly, failing the required downwards ramp rate of 10%/min. It also can be seen that once the front passes by, instant power increases beyond the allowed upwards ramp. In a day with medium clearness index and high wind speed like the one shown in the figure, this process occurs time after time. That leads to the question of the size of the corresponding battery, in terms of power and energy capacity, for accomplishing such regulations. These requirements are given by both PV power downwards and upwards fluctuations that exceed a given ramp rate limitation, evaluating required battery power, $P_{BAT}(t)$, and energy, E_{BAT}, for each fluctuating event. Fig. 2 shows a sample of these events and battery power and energy requirements to manage them.

In previous works, procedures have been proposed to characterise PV power fluctuations and to size batteries for complying with a certain power ramp rate limitation. An appropriate short term PV power variability analysis is necessary for describing the behaviour of a PV plant under intermittent irradiance conditions, for detecting the problems that it could cause to the grid. In this context, several techniques have been used in the literature. While early studies characterised irradiance variability (Tomson and Tamm, 2006; Woyte et al., 2007), currently statistical methods are used for effectively characterising PV plant output power fluctuations (Hoff and Perez, 2010; Marcos et al., 2011a, 2011b; Mazumdar et al., 2014; Mills et al., 2009; Van Haaren et al., 2014).

Despite part of the fluctuations can be smoothed by geographically dispersing PV plants (Lave et al., 2012; Marcos et al., 2012; Murata et al., 2009), strict grid regulations demand buffering

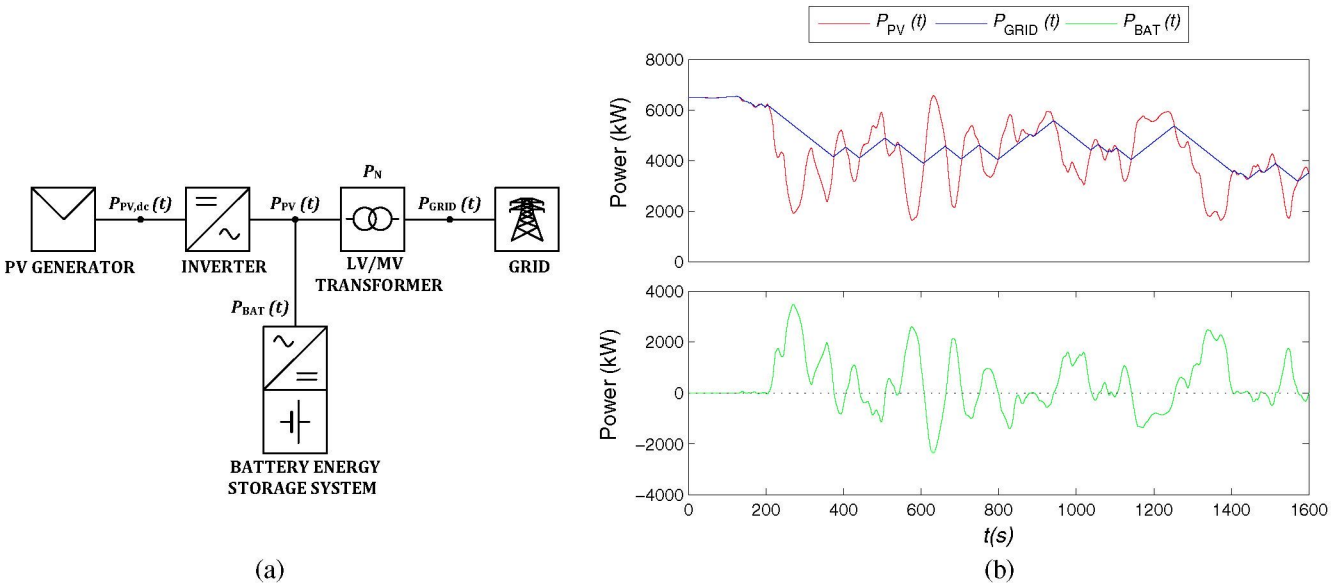

Fig. 1. PV power fluctuations smoothing by means of BESS. (a) The battery is connected in the point of common coupling (PCC) in order to absorb PV power fluctuations and to inject power to the grid, $P_{GRID}(t)$, in a required 10%/min ramp rate (b). In a day with medium clearness index and high wind speed, downwards and upwards fluctuations occur time after time.

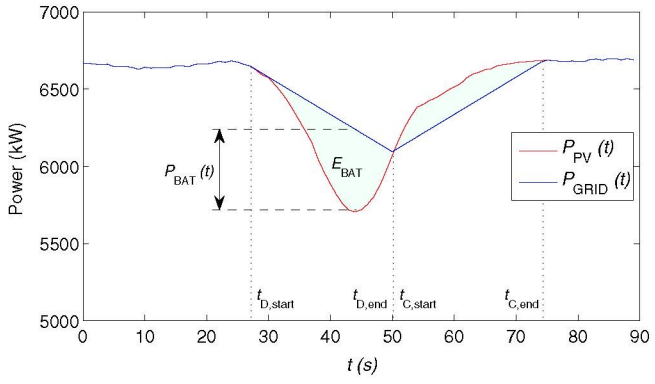

Fig. 2. $P_{GRID}(t)$ is modulated following the prescribed RR limit. When a cloud passes over the plant and $P_{PV}(t)$ decreases below RR_{LIM}, battery is discharged at a certain power $P_{BAT}(t)$ supplying required energy E_{BAT}. When the cloud is gone and $P_{PV}(t)$ is recovered faster than RR_{LIM}, the battery absorbs excess power and extra energy is stored in it. Both discharge and charge events start ($t_{D,start}$ and $t_{C,start}$) when $P_{PV}(t)$ exceeds RR_{LIM} and end when either fluctuation sign changes ($t_{D,end}$) or when RR_{LIM} is kept again ($t_{C,end}$).

capabilities to individual PV plants. By analysing PV powers fluctuations statistically, in Perez and Hoff, 2013; van Haaren et al., 2015 the fluctuations mitigation is addressed by means of energy storage systems. In line with this and based on one second long-term observations at PV plants of different sizes, a model for the "worst fluctuation" (WF) was proposed in Marcos et al., 2014b. Roughly, it corresponds to the darkening of the PV array (from clear sky irradiance to diffuse irradiance) by a cloud moving at about 80–90 km/h, which is also confirmed by Lave and Kleissl, 2013. Providing the battery can be fully recharged between two consecutive fluctuations by means of a state of charge (SOC) driven control, the WF model allows sizing the battery for full compliance of ramp-rate limits (Marcos et al., 2014a).

However, adhering exclusively to ramp rate control requirements, that leads to rather large and expensive batteries which are likely impractical because such worst fluctuation seldom occurs and even in case of occurrence its consequences are not necessarily catastrophic. Although, batteries are undergoing an intense development in their technological features, leading them to a fall in their cost (Gallagher et al., 2011; Wood et al., 2015; Yoo et al., 2014), they are still rather expensive. As a consequence, smaller batteries, able to absorb the majority but not all the fluctuations, are likely more practical. In this context, some authors have pointed out the need of reducing the storage requirements for ramp rate applications. For instance, in van Haaren et al. (2015) the authors proposed two algorithms for smoothing power fluctuations, simulating ramp rate failures of a PV plant with different storage sizes up to smoothing 99% of fluctuating events.

However, there is a gap in the current state of the art about the analysis of size reduction for different ramp rate limits and power data sampling requirements. It is necessary to deeply address the effects of limiting the battery power and energy capacity requirements, which would allow boosting the economic feasibility of using them in large PV plants. This paper addresses the sizing of practical batteries by taking into consideration, both, the fluctuation occurrence and the penalties in case of non-compliance of the prescribed ramp-rate limitations. In this context, the objective of the work is double:

- To model the ramp rate limit failures derived from the reduction of battery power and capacity requirements, considering different ramp rate limits and the sampling time used for evaluating it.
- To apply the battery reduction analysis to the Puerto Rico grid-code requirements, taking into account the specific conditions and power curtailments imposed as penalty.

In order to achieve these objectives, the paper is structured as follows. On the one hand, in Section 2 the relation between battery size reduction and ramp rate compliance is analysed in a theoretical way. First, the method used for analysing the battery size reduction and the data used as input for extensive simulation is described. Then, the contributions of the analysis are presented as results.

On the other hand, in Section 3 a case study is presented applying the battery reduction analysis, explaining first the applied methodology and second the results derived from the analysis.

2. Relation between battery size and ramp-rate limitation compliance

A ramp is defined by the sudden variation of the output of a PV plant caused by an irradiance fluctuation. When power output falls suddenly due to cloud cover, a ramp occurs. The rate of change of power output due to an irradiance fluctuation which lasts a specific duration, is called the facility's ramp rate (RR) and it can be expressed as a percentage of the plant's nominal power per unit of time differential, defined in Eq. (1).

$$RR = \frac{[P_{PV}(t) - P_{PV}(t - \Delta t_R)]/P_N}{\Delta t_R} \quad (1)$$

where $P_{PV}(t)$ is the PV plant output power at a given instant t, P_N is the PV plant nameplate power capacity and Δt_R is the time differential of the ramp rate, typically equalling to 1 min.

2.1. Method for calculating P_{BAT} and E_{BAT} series and battery size

Fig. 3 shows a typical downwards PV power fluctuation caused by a cloud passing over a PV generator and the corresponding evolution of the power required from the battery to preserve a given ramp-rate limitation, RR_{LIM}. For a given fluctuation, battery power, $P_{BAT}(t)$, is given by the difference between allowable power to be injected to the grid, $P_{GRID}(t)$, and the power from the PV plant, $P_{PV}(t)$. $P_{GRID}(t)$ is calculated as an increase or decrease of PV power limited to the maximum allowable variation, ΔP_{RR}, in each studied time step. This is described by Eqs. (2)–(4). Considering Δt the time step of the analysed production data series, the ramp rate defined in Eq. (1) is adapted to each step. The process is the same for upwards fluctuations, but in this case with the opposite sign. As a matter of convenience, battery discharge (downwards fluctuation) is considered as positive $P_{BAT}(t)$, while battery charge (upwards fluctuation) is considered as negative $P_{BAT}(t)$.

$$\Delta P_{RR} = P_N \cdot \frac{RR_{LIM}}{\Delta t_R/\Delta t} \quad (2)$$

$$P_{GRID}(t) = P_{GRID}(t - \Delta t) + \min(P_{PV}(t) - P_{PV}(t - \Delta t), \Delta P_{RR}) \quad (3)$$

$$P_{BAT}(t) = P_{GRID}(t) - P_{PV}(t) \quad (4)$$

Extending the exercise along a representative period (one full year in our case), yields the time series of required battery power of every fluctuation event. The nominal battery power requirement for full ramp rate compliance, $P_{BAT,MAX}$, is calculated as the maximum of the $P_{BAT}(t)$ time series, defined in Eq. (5).

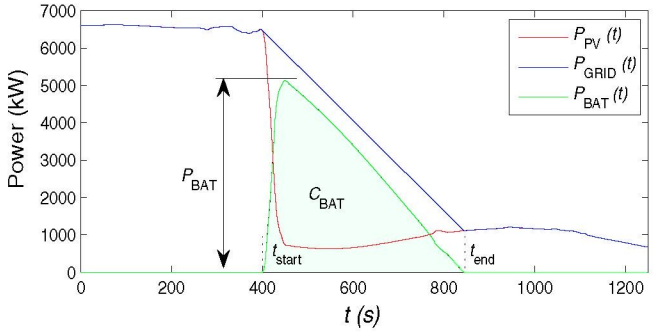

Fig. 3. Battery power and capacity characterisation in order to comply with a given RR and smooth fluctuations. The displayed downwards fluctuation starts at $t_{start} = 400$ s and stops at $t_{end} = 850$ s and it represents the maximum battery power ($P_{BAT} = 5132$ kW) and capacity ($C_{BAT} = 336$ kW h) requirement of a 7.243 MW PV plant in northern Spain observed in a particular year, for $RR = 10\%$/min.

$$P_{BAT,MAX} = \max(|P_{BAT}(t)|) \quad (5)$$

The energy managed by the battery during each downwards (upwards) fluctuation is calculated by the integral of the battery power curve defined between the limits of each discharge (charge) event, $t_{D,start}$ and $t_{D,end}$ ($t_{C,start}$ and $t_{C,end}$) respectively as shown in Fig. 2. Note that, despite the downwards-upwards symmetry of the PV power, the net annual energy flow from the battery is negative, i.e. the battery SOC decreases. Because of that, a battery managed just to absorb PV power fluctuations tends to progressively discharge along the year. However, it has been shown that such loss of charge can generally be compensated by recharging the battery from the PV array before the next fluctuation occurs (de la Parra et al., 2015; Marcos et al., 2014a). We will here adhere to this practice, because it just minimizes the battery size requirements. Hence, the energy requirement E_{BAT} for absorbing a complete fluctuation event, either downwards or upwards fluctuation, is given by the following equations, where D or C define a battery discharge or charge operation respectively.

$$E^D_{BAT} = \int_{t_{D,start}}^{t_{D,end}} P_{BAT}(t)dt \quad (6)$$

$$E^C_{BAT} = \int_{t_{C,start}}^{t_{C,end}} P_{BAT}(t)dt \quad (7)$$

The series of battery energy requirements for each discharge and charge event are calculated by integrating the battery power along each fluctuation event, defined as the period between two consecutive battery power changes of sign. The maximum value of discharge events, $E^D_{BAT,MAX}$, represents the maximum energy supplied by the battery during the most energy-restrictive downwards fluctuation, while the absolute value of the minimum of charge events, $\left|E^C_{BAT,MIN}\right|$, is the maximum energy stored in the battery during the most energy-restrictive upwards fluctuation. The finally required battery energy capacity for full ramp rate limitation compliance, $C_{BAT,MAX}$, is given by the maximum of both discharge and charge energy requirement values, defined in Eq. (8).

$$C_{BAT,MAX} = \max\left(E^D_{BAT,MAX}, \left|E^C_{BAT,MIN}\right|\right) \quad (8)$$

However the energy capacity requirement also depends on the implemented control algorithm. Implementing a SOC control algorithm in the simulation, which means that consecutive fluctuations are considered as independent, then the energy requirements of discharge and charge events can be considered independently. This algorithm restores the battery to SOC = 50% before the start of every new fluctuation, being able to discharge it completely to smooth a sudden maximum downwards fluctuation, or on the contrary to leave enough capacity to charge the excess of a maximum upwards fluctuation. For this particular algorithm, this is achieved by doubling $C_{BAT,MAX}$.

For a given RR and Δt combination, the study of battery reduction is carried out by analysing the histogram of the resulting battery power time series and the histogram of the resulting series of battery energy requirements for each event.

2.2. Experimental data

An extensive simulation exercise was performed using as input one second power values recorded at a 7.2 MW PV power plant located in Milagro, northern Spain. The plant under analysis is equipped with vertical axis trackers covering an area of 52 Ha. High quality PV plant output power data was collected by means of a power meter at the point of common coupling and recorded by a PLC.

Besides, other relevant parameters such as horizontal and tilted irradiance was measured by calibrated modules and recorded by the PLC. Irradiance data was really useful in order to detect some power measurement errors. At first glance, some sudden power decays were detected in the dataset, which were initially studied as ramps because they were not identified as data logging common faults. However, after comparing irradiance and power data, they turned out to be errors and were filtered out from the dataset. For instance, an inverter of a certain PV plant section can suffer a sudden disconnection fault and the subsequent reconnection, which can resemble a power ramp. The irradiance-power data correspondence process prevents us from sizing the battery for erroneous ramps.

2.3. Results and discussions

(a) Battery size for 100% fluctuations smoothing

In most cases, given the high value of the maximum power, it makes sense to suppose that $P_{BAT,MAX}$ and $C_{BAT,MAX}$ will correspond to the same fluctuation event. For instance, Fig. 3 shows an event in which maximum power and energy requirement of the year are fully used, in this case discharging. However, this is not necessarily always like this, as energy requirement also depends on the length of the event. Therefore both power and capacity sizing must be calculated independently. For a given PV plant and location, the result of this exercise depends on the values of RR_{LIM} and Δt. Given that $P_{PV}(t)$ data were recorded with one second sampling time, we can extend the exercise to any Δt being multiple of 1 s, depending on the monitoring requirements of each particular grid-code. Table 1 shows $P_{BAT,MAX}$ and $C_{BAT,MAX}$ values for absorbing 100% of fluctuations of the studied year, in order to comply with *RR* limits of 5, 7.5, 10, 20 and 30%/min and considering Δt = 2 s.

(b) Calculation of histograms of P_{BAT} and E_{BAT} series

In order to generalise the model for its suitability along different years, instead of using the full battery sizing expressions of Eqs. (5) and (8), the maximum battery power requirement, $P_{BAT,WF}$, and battery energy capacity requirement, $C_{BAT,WF}$, values are used, given by the so called "worst fluctuation model", WF (Marcos et al., 2014b). These design values are displayed in Table 2.

As it can be seen, the values are similar to the ones obtained in the previous section. Most of the values of Table 1 are slightly lower because they are derived from the fluctuations of a single year, while WF model describes the worst case possible. It is worth mentioning that depending on the control algorithm applied to the operation of the battery, the battery capacity $C_{BAT,WF}$ should be doubled, as explained in Section 2.1. However, there are methods for avoiding this, for example by absorbing the upwards fluctuations moving the operation point of the plant inverters out of the MPP, which involves some PV energy loss virtually insignificant. However, this issue is not covered by this paper and for a more detailed discussion on the relation between battery capacity, control strategies and energy loss the reader is addressed to references de la Parra et al. (2016, 2015) and Ina et al. (2004). The present work is focused on the relation between ramp rate compliance and battery size reduction, analysing statistically the power and energy requirements of every downwards and upwards fluctuation event as a fraction of reference values, i.e. $P_{BAT,WF}$ and $C_{BAT,WF}$ of Table 2.

Table 1
Battery size for full compliance of different ramp rate limits at Milagro PV plant.

RR in %/min	Power in kW (*% of* P_N)	Capacity in kWh (*min*)
5	5447 (*75.21*)	765 (*6.3*)
7.5	5287 (*73*)	471 (*3.9*)
10	5132 (*70.86*)	336 (*2.78*)
20	4634 (*64*)	160 (*1.3*)
30	4170 (*57.6*)	95 (*0.8*)

Table 2
Battery size for full compliance of different ramp rate limits at Milagro PV plant, as given by the Worst Fluctuation Model.

RR in %/min	Power in kW (*% of* P_N)	Capacity in kWh (*min*)
5	5713 (*78.9*)	925 (*7.7*)
7.5	5416 (*74.8*)	600 (*5*)
10	5148 (*71.1*)	437 (*3.6*)
20	4262 (*58.8*)	192 (*1.6*)
30	3558 (*49.1*)	111 (*0.9*)

For analysing battery size reduction, 10 iterative simulations were carried out, one for each *RR* and Δt combination, obtaining the respective P_{BAT} and E_{BAT} series as explained in Section 2.1. If we split into bins of a histogram the resulting data of battery power or energy series, we can define certain power or energy intervals. For the whole series, any P_{BAT} and E_{BAT} of any fluctuation event lies in between one of those intervals, considering them as fractions of full size $P_{BAT,WF}$ and $C_{BAT,WF}$, defined in Eqs. (9) and (10):

$$P_{BAT} = k_p \cdot P_{BAT,WF} \tag{9}$$

$$E_{BAT} = k_c \cdot C_{BAT,WF} \tag{10}$$

where k_p and k_c are the interval limits ranging from 0 to 1. The core purpose is to predict the occurrence of battery power and energy values along the year higher than P_{BAT} and E_{BAT}, with which the reduced battery could not cope.

Fig. 4 shows for a full year the histograms of P_{BAT} and E_{BAT}, for *RR* values of 5, 7.5, 10, 20 and 30%/min and Δt values of 2 s and 30 s. For the sake of simplicity, only discharge power (left) and energy (right) histograms have been displayed (downwards fluctuations) and the explanation will focus on these parameters. However, histograms of P_{BAT} and E_{BAT} for upwards fluctuations have also been analysed with the same method.

Moreover, looking for presentation clarity, the histograms of Fig. 4 consider only the range higher than a threshold $u = 0.1\%$, ($P_{BAT} > u \cdot P_{BAT,WF}$ and $E_{BAT} > u \cdot C_{BAT,WF}$). This makes sense as it corresponds to neglecting signal values below the measurement equipment resolution.

This way, normalising these distributions to their respective integrals on the interval [u, 1] equalling to 1, cumulative frequencies for any given P_{BAT} can be calculated, which can be understood as the conditional probability density functions of P_{BAT} given $P_{BAT} > u$. In turns, the probability of $P_{BAT} > u$ is given by the ratio between the time the battery is operating beyond the threshold to the total time the battery is operating, $T_{P_{BAT}>u}/T_{P_{BAT}>0}$. This ratio also depends on applicable *RR* and Δt.

(c) Analytical expressions of distributions

Looking for an analytical expression for the histograms of Fig. 4, it was found that the most appropriate fit was an exponential function as the one described in Eq. (11). It keeps a good balance between a high goodness of fit and simplicity. The goodness of the fit of each *RR* - Δt combination distribution is proven later on in Table 3 with its respective R^2 index.

$$f(x)_{|P_{BAT}>u} = ae^{-bx} \tag{11}$$

In the case of power distribution, x corresponds to the power fraction $P_{BAT}/P_{BAT,WF}$. Assuming $u \ll 1$ and given that the area below each frequency distribution equals to 1:

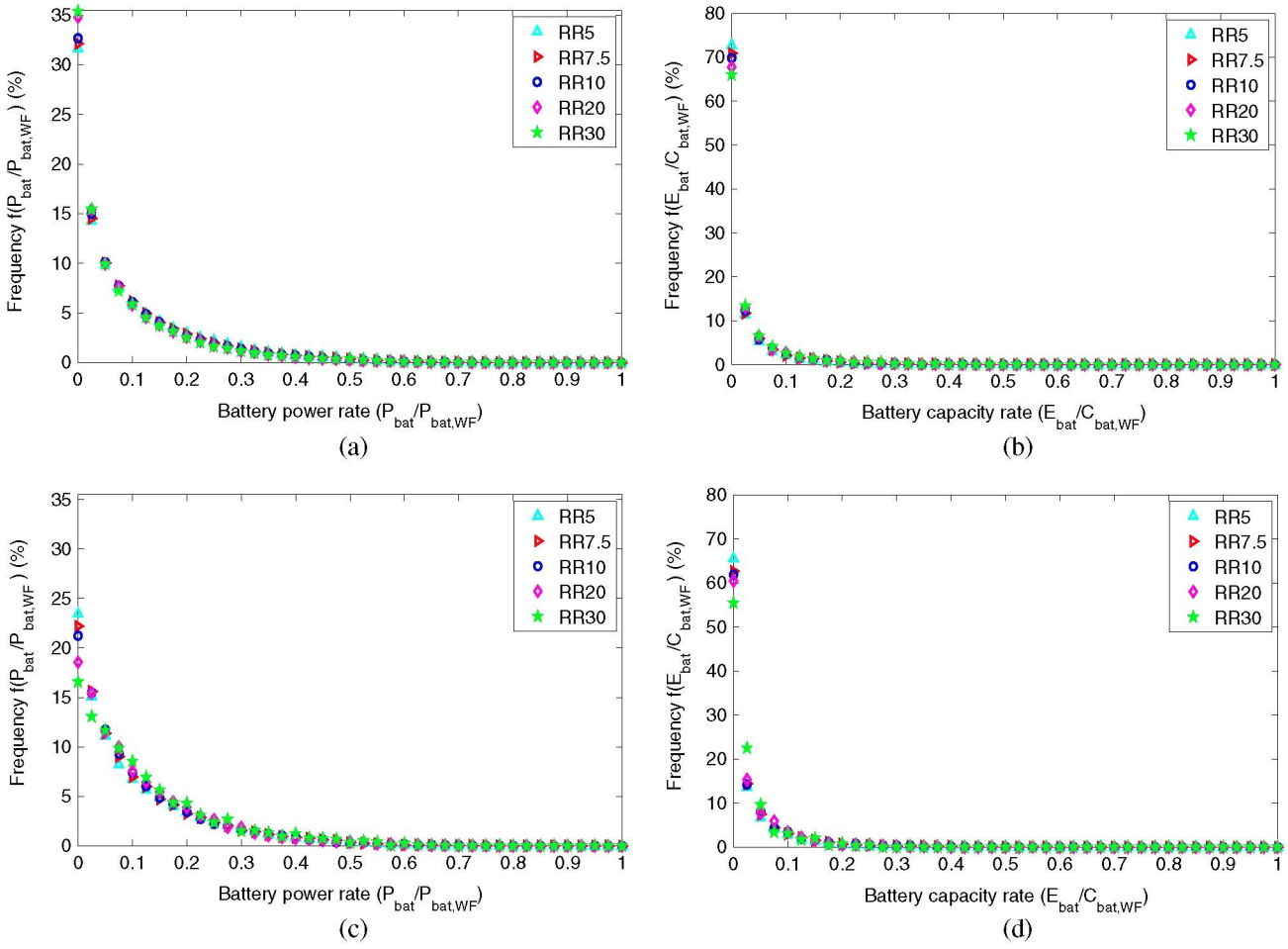

Fig. 4. Battery discharge power (left) and energy (right) histograms along a full year, for RR = 5, 7.5, 10, 20 and 30%/min and for Δt = 2 s (a, b) and Δt = 30 s (c, d).

Table 3
Curve fitting parameter and goodness of fit index for each RR_{LIM} and Δt combination.

Δt	Fit	RR (% P_N/min)									
		P_{BAT} (discharge)					E_{BAT} (discharge)				
		5	7.5	10	20	30	5	7.5	10	20	30
2	b	17.57	17.63	18.08	20.31	21.15	69.56	66.62	64.38	60.54	58.05
	R^2	0.948	0.952	0.956	0.960	0.960	0.995	0.993	0.993	0.993	0.992
30	b	10.54	9.92	9.41	8.20	7.10	56.82	52.03	51.09	47.49	35.07
	R^2	0.980	0.990	0.995	0.998	0.997	0.991	0.990	0.988	0.987	0.998

$$F(x=1)_{|P_{BAT}>u} = \int_u^1 f(x)_{|P_{BAT}>u} dx = a\int_u^1 e^{-bx}dx = \frac{a}{b}(e^{-bu}-e^{-b}) \approx \frac{a}{b}e^{-bu} = 1 \rightarrow a = be^{bu} \quad (12)$$

Resulting in a simplification of Eq. (11) to only one parameter:

$$f(x)_{|P_{BAT}>u} = be^{-b(x-u)} \quad (13)$$

Table 3 shows the curve fitting parameter b and the goodness of the fit for each histogram of every combination of RR and Δt. As it can be seen, R^2 values range between 0.948 and 0.998.

(d) Model of ramp rate limitation non-compliance as a function of the battery size

The model could be used as a frequency distribution tool to predict with good accuracy the occurrence of a certain battery power and the energy managed by the battery during a fluctuation event. As a consequence, the cumulative frequency of a certain charge power value of being higher than a given $P_{BAT}/P_{BAT,WF}$ fraction, defined as k_p, is given by integrating Eq. (13) defined in the range higher than this fraction. Note that $u \ll 1$ assumption is also taken into account, which results in an easy analytical expression.

$$F(x>k_p)_{|P_{BAT}>u} = \int_{k_p}^1 f(x)_{|P_{BAT}>u} dx = \int_{k_p}^1 be^{-b(x-u)}dx = e^{-b(k_p-u)} \quad (14)$$

The previous equation is also valid for expressing charge power cumulative frequency and even for discharge or charge energy cumulative frequency, using appropriate b parameter in each case and replacing k_p with k_c in the cases of energy. Note that Eq. (14) represents the conditional probability given $P_{BAT} > u$. In order to calculate the total probability related to the time when PV plant is injecting power, it is necessary to take into account the battery discharging time supporting downwards fluctuations and the

battery discharging time beyond the threshold u. These time periods are defined in Table 4 while their relationship as operating factors, for different RR and Δt, are explained in Table 5. These tables include the definitions for charge power times. Subscript d is used in operating factors for discharge and c is used for charge.

So, total probability of occurrence of an instant with battery discharge power higher than a given reduced fraction k_p is calculated by means of the following expression:

$$F(x > k_p) = OF_d \cdot OF_{d,u} \cdot F(x > k_p)_{|P_{BAT}>u} = OF_d \cdot OF_{d,u} \cdot e^{-b(k_p-u)} \quad (15)$$

However, the previous equation cannot be directly used for capacity reduction analysis. Operating factor parameters of Table 4 are calculated by taking into account battery operating times against PV plant production times. It means that the cumulative frequency is defined for the time domain, representing the probability of occurrence of a battery power requirement higher than k_p in a given PV power generating instant of the year. But battery energy histogram is defined for discharge (charge) events rather than for time domain. Like this, each discharged (charged) energy amount is associated to a single fluctuation event, being the frequency distribution related to the total amount of fluctuation events of its type. Consequently, the approach for capacity reduction analysis is different. The model will give a probability of occurrence of an event with a required capacity higher than a given $E_{BAT}/C_{BAT,WF}$. In other words, it gives information about how likely it is not to have enough capacity for absorbing the complete fluctuation event, once immersed in it. Eq. (16) describes the probability for discharging energy events (downwards fluctuations). In order to consider only significant energy flows higher than the threshold u, the fraction of the significant events observed in the studied year, SF, is applied to Eq. (14). Significant events description and significant events fractions for different RR and Δt are shown in Tables 6 and 7 respectively. Subscript d is used for fractions of discharge events and c is used for charge ones.

$$F(x > k_c) = SF_d \cdot F(x > k_c)_{|E_{BAT}>u} = SF_d \cdot e^{-b(k_c-u)} \quad (16)$$

Table 4
Yearly PV plant and battery operation periods.

Period	Description
T_D	Time while PV plant is generating (4084 h)
$T_{P_{BAT}\neq 0}$	Oscillating time, battery is operating
$T_{P_{BAT}>0}$	Battery discharging time, downwards fluctuations
$T_{P_{BAT}<0}$	Battery charging time, upwards fluctuations
$T_{P_{BAT}>u}$	Battery discharging time, beyond threshold
$T_{P_{BAT}<-u}$	Battery charging time, beyond threshold

Table 6
Significant battery energy events definition, with energy transfer beyond threshold u.

Significant events	Description
$E_{BAT} > u$	Events with discharged energy beyond threshold
$E_{BAT} < -u$	Events with charged energy beyond threshold

The results of the model are in accordance to previous studies carried out, both in terms of fluctuations characterisation and in terms of battery size assessment for facing them. The battery requirements model developed in the present study follows an exponential function similar to the one developed in Marcos et al. (2011b) for fluctuations description. This makes sense, as the battery size reduction is correlated with the fluctuations size and their occurrence. In a similar way, the model also follows the exponential behaviour of the non-compliances function described in van Haaren et al. (2015), for both battery power and capacity requirements of a PV plant with a nameplate power capacity similar to the one used in this work.

(e) Example of application

Finally, as an illustrative example, in Tables 8and 9 the probability of not complying with different ramps with certain reduced battery is explained. In terms of battery discharge power for downwards fluctuations, the probability of incurring in instants with battery power requirements higher than 10% and 20% of $P_{BAT,WF}$ is shown in Table 8, both as conditional probability given that power is higher than u and as total probability. In terms of battery discharge capacity, the probability of a discharge event to need more capacity than 5% and 10% of the design battery capacity $C_{BAT,WF}$ is shown in Table 9. Again, left part of the table shows the conditional probability for discharge events with $E_{BAT} > u$, while right part is the total probability for every discharge event. In order to have a global view, the exercise has also been extended to power charge instants and energy charge events, not included here for simplicity reasons.

The model proves that the potential for reducing the battery size given by the worst fluctuation model is high. The number of failures in terms of RR limitation compliance of a battery with a power 20% of $P_{BAT,WF}$ and a capacity 10% of $C_{BAT,WF}$ is scarce, following the low occurrence of sudden fluctuations.

3. Case study: Optimal battery size in Puerto Rico considering penalties

Taking into account current grid codes, optimal battery size from the PV plant owner viewpoint results from a trade-off between battery investment costs and applicable penalties in case

Table 5
Yearly battery operating factors for 2 s and 30 s sampling time and 5, 7.5, 10, 20 and 30%P_N/min ramp rate limitations.

Operating factors	Δt	RR (% P_N/min)				
		5	7.5	10	20	30
$OF = \frac{T_{P_{BAT}\neq 0}}{T_D}$	2	0.229	0.167	0.128	0.054	0.026
	30	0.175	0.121	0.088	0.030	0.012
$OF_d = \frac{T_{P_{BAT}>0}}{T_D}$	2	0.116	0.085	0.065	0.027	0.013
	30	0.089	0.062	0.045	0.015	0.006
$OF_c = \frac{T_{P_{BAT}<0}}{T_D}$	2	0.113	0.083	0.063	0.027	0.013
	30	0.086	0.059	0.043	0.015	0.006
$OF_{d,u} = \frac{T_{P_{BAT}>u}}{T_{P_{BAT}>0}}$	2	0.925	0.937	0.950	0.957	0.963
	30	0.986	0.988	0.989	0.990	0.990
$OF_{c,u} = \frac{T_{P_{BAT}<-u}}{T_{P_{BAT}<0}}$	2	0.920	0.933	0.946	0.957	0.964
	30	0.986	0.988	0.990	0.991	0.994

Table 7
Significant battery energy events fraction, for 2 s and 30 s sampling time and 5, 7.5, 10, 20 and 30%P_N/min ramp rate limitations.

Significant events fraction	Δt	*RR* (% P_N/min)				
		5	7.5	10	20	30
$SF_d = \frac{E_{BAT>u}}{E_{BAT>0}}$	2	0.372	0.437	0.475	0.537	0.574
	30	0.780	0.848	0.889	0.951	0.971
$SF_c = \frac{E_{BAT<-u}}{E_{BAT<0}}$	2	0.366	0.439	0.476	0.542	0.587
	30	0.758	0.826	0.880	0.947	0.982

Table 8
Probability of occurrence of non-compliances with two different battery power fractions, relative and absolute.

$P_{BAT}/P_{BAT,WF}$	Δt	$F(x > k_p)_{\|P_{BAT}>u} \cdot 100(\%)$					$F(x > k_p) \cdot 100(\%)$				
		5	7.5	10	20	30	5	7.5	10	20	30
0.1	2	17.6	17.5	16.7	13.4	12.3	1.9	1.4	1.0	0.4	0.2
	30	35.2	37.4	39.4	44.4	49.5	3.1	2.3	1.8	0.7	0.3
0.2	2	3.0	3.0	2.7	1.8	1.5	0.3	0.2	0.2	0.1	0.0
	30	12.3	13.9	15.4	19.6	24.3	1.1	0.9	0.7	0.3	0.1

Table 9
Probability of occurrence of non-compliances with two different battery capacity fractions, relative and absolute.

$E_{BAT}/C_{BAT,WF}$	Δt	$F(x > k_c)_{\|E_{BAT}>u} \cdot 100(\%)$					$F(x > k_c) \cdot 100(\%)$				
		5	7.5	10	20	30	5	7.5	10	20	30
0.05	2	3.3	3.8	4.3	5.2	5.8	1.2	1.7	2.0	2.8	3.3
	30	6.2	7.8	8.2	9.8	17.9	4.8	6.6	7.3	9.3	17.4
0.1	2	0.1	0.1	0.2	0.2	0.3	0.0	0.1	0.1	0.1	0.2
	30	0.4	0.6	0.6	0.9	3.1	0.3	0.5	0.6	0.9	3.0

of non-compliance with *RR* regulations. The larger the battery size, the larger the compliance. Hence, the cheaper the unitary cost of battery and the larger the penalties are, the larger the optimal battery is.

The only penalties proposal known to date is included in the regulation prepared by the Puerto Rico Electric Power Authority (PREPA). This organisation has established minimum technical requirements (MTR) for interconnection of photovoltaic power plants, developed and complemented with the support of different public authorities like US Department of Energy, NREL and the association of renewable energy producers of Puerto Rico (APER) (Gevorgian and Booth, 2013; PREPA, 2012). Despite they are out of the scope of this article, it is worth mentioning that the code includes other features apart from RR limitations. It gives specifications about voltage fault ride-through and short-circuit ratio, frequency ride-through and frequency response, power quality criteria and voltage and reactive power regulation through power factor.

In the particular case of RR limitation, the proposal considers penalties through PV power curtailment for complete week periods, as a function of RR non-compliance observed the week before. This code limits the RR to 10%/min. For this scenario, the application of the battery size reduction assessment will be carried out taking into consideration the specific conditions, adapting the simulation process accordingly.

3.1. Methodology

The simulation implements a SOC control algorithm explained in Section 2.1, with the full size battery power and capacity reference values given by the WF model (Table 2) and corresponding to $P_{BAT,WF}$ and $2 \cdot C_{BAT,WF}$ respectively. Therefore, a full size battery will operate up to a maximum rated $P_{BAT,WF}$ in each fluctuation event. However, the capacity reserved at the beginning of each type of fluctuation (downwards or upwards) will be $C_{BAT,WF}$, i.e. half of the reference capacity for each type.

The regulation proposal includes a practical implementation procedure consisting on the following steps:

(a) PV plant injected power monitoring

P_{GRID} is scanned at 2 s rate ($\Delta t = 2$ s) during all the time the PV plant is injecting power into the grid.

(b) Ramp rate compliance evaluation of the scans

For each scan, the ramp rate compliance, *RRC*, is evaluated with a scan differential method for measuring the RR. For example, a *RR* of 10%/min will be traduced to 10%/30 for $\Delta t = 2$ s, evaluating accordingly every 2 s scan of an entire week during producing hours of the plant. Like this, for every week both compliant and non-compliant scans are aggregated to calculate weekly RRC.

Reducing the battery power in a certain magnitude k_p will prevent the battery from absorbing some fluctuations, lowering RRC of the scans involved in them. If the required instant power $P_{BAT}(t)$ (see Eq. (4)) to be managed by the battery in either downwards or upwards fluctuations exceeds its reduced power (Eq. (9)), the step is non-compliant for power (NC_P), which is done evaluating the following expression:

$$|P_{BAT}(t)| \geqslant P_{BAT,WF} \cdot k_p \tag{17}$$

The weekly non-compliance grade of the PV plant in terms of power $NC_P(\%)$ is obtained expressing the non-compliant scans as a percentage of total scans during generation periods, N_{ON}.

$$NC_P(\%) = 100 \cdot \frac{NC_P}{N_{ON}} \tag{18}$$

Reducing battery capacity by a certain magnitude k_c will prevent the battery from absorbing some fluctuations, lowering RRC. The analysis counts the battery energy flow of every 2 s step by integrating $P_{BAT}(t)$ in every fluctuation (see Eqs. (6) and (7)). If the cumulative sum of the energy of every step at a point of the fluctuation overflows the reduced battery capacity (Eq. (10)), either in a charge or discharge process, this step (and as a consequence the rest of the following steps of the fluctuation) will be marked as non-compliant for capacity (NC_C). This process is cumulative, which means that for a step which lasts from $t = n$ to $t = n + \Delta t$, all energy managed previously since the start of the fluctuation ($t = 0$) must be considered. This is evaluated with the following equation:

$$\left| \int_0^t P_{BAT}(t)dt + \int_t^{t+\Delta t} P_{BAT}(t)dt \right| \geqslant C_{BAT,WF} \cdot k_c \tag{19}$$

The weekly non-compliance grade of the PV plant in terms of capacity $NC_C(\%)$ is obtained expressing the number of non-compliant scans as a percentage of total scans during generation periods.

$$NC_C(\%) = 100 \cdot \frac{NC_C}{N_{ON}} \tag{20}$$

(c) Weekly RRC calculation

For each week, a RR compliance index (RRC_w) is calculated with the following expression:

$$RRC_w(\%) = 100 \cdot \left(1 - \frac{NC}{N_{ON}}\right) \tag{21}$$

where NC is the number of non-compliant scans, obtained adding NC_P and NC_C scans and being careful of not adding twice a single scan that is simultaneously non-compliant in terms of power and capacity.

(d) Weekly curtailments calculation

In the particular case of Puerto Rico, there are linked dynamics of RRC and curtailment which justify the need of a weekly assessment of the effects derived from reducing battery size, instead of the annual analysis explained in Section 2. Due to statistical factors such as tolerance, metering accuracy or latency, the weekly minimum compliance to avoid curtailments is proposed as $RRC_{min} = 98.5\%$. Consequently, if in a weekly basis less than 98.5% of the production scans comply with the proposed RR, grid operator will impose a curtailment for the next week. Curtailments of a given week Cu_w are as follows:

$$Cu_w = (Cu_{w-1} - (RRC_{\min} - RRC_{w-1})) \tag{22}$$

$$P_{PV,w} = P_N \cdot Cu_w \tag{23}$$

where Cu_{w-1} and RRC_{w-1} are respectively the curtailment and ramp rate compliance calculated for the previous week, while $P_{PV,w}$ is the weekly maximum injection power. Note that the curtailment factor is cumulative; which means that for correcting it for a given week, previous week RRC must be better than the minimum one. As a result, $P_{PV,w}$ for each week is calculated applying the correspondent curtailment factor to the PV plant nominal power P_N.

(e) Yearly PV energy calculation

In order to evaluate the effect of combining both battery power reduction and capacity reduction, the most objective indicator is the yearly produced PV energy. This value is obtained performing a yearly simulation for each k_p and k_c combination. Assessing RRC and the involved curtailments along the full year of each simulation, the power injected into the grid for each combination of k_p and k_c, $P_{GRID,k_p,k_c}(t)$ is obtained. Integrating each of these time series for the total scans of the year n, total yearly energy injected to the grid for every combination is obtained.

$$E_{GRID,k_p,k_c} = \int_0^n P_{GRID,k_p,k_c}(t)dt \tag{24}$$

This parameter is useful for selecting a proper combination of k_p and k_c.

3.2. Results and discussions

Fig. 5 illustrates the linked dynamics of RRC and curtailment corresponding to the same Milagro PV power time series of the previous section, using a battery whose power is just 10% of $P_{BAT,WF}$. Fig. 5a shows the $P_{PV}(t)$ evolution along a day of week 31 (last week of July 2009) without (blue) and with $Cu_{31} = 60\%$ weekly curtailment factor (red[1]). This value results from the previous week RR compliance, RRC_{30}, and the accumulated Cu_{30} (week 30: $RRC_{30} = 97.5\% | Cu_{30} = 0.61$). From the beginning of the year, the accumulated curtailment dropt to $Cu_{30} = 61\%$, so adding the 1% of under-compliance incurred in week 30, Cu_{31} is reduced in this amount. Fig. 5b shows the corresponding battery power required for full RRC of that week at full available $P_{PV}(t)$ (blue) and if plant injects with curtailed limit of $P_{PV,31}$ (red). The direct link between curtailment and RR compliance becomes evident. Battery requirements for full RR compliance are lower for the curtailed PV plant than for the non-curtailed one. Fig. 5c and d show yearly evolution of RRC and power curtailment.

Fig. 6 shows the corresponding evolution of weekly energy loss, caused by reducing P_{BAT} to 10% of $P_{BAT,WF}$ and keeping full $C_{BAT,WF}$, with respect to maximum generation obtained with full power battery. Fig. 6b makes evident that the loss evolution follows the curtailment imposed as shown in Fig. 5d.

Therefore, some loss limits must be established in order to clear up the way for business models with a balance between cost savings derived from battery size reduction and incomes reduction owing to production loss. Fig. 7 extends the simulation exercise to different power and capacity battery sizes, showing, for every k_p and k_c combination, the annual energy loss with respect to full battery size. The first relevant result obtained from this graph is that there is no energy loss beyond 30% $P_{BAT,WF}$ - 15% $C_{BAT,WF}$ combination, placed in the corner. Reducing below these limits, the losses increase exponentially. It is also worth mentioning that if one of the parameters is kept high, the other one can be slightly reduced below those limits without any additional energy loss. Moreover, it is shown that the losses are limited to around 48.7% of the maximum generation. However, it makes sense to affirm that the grid operator should not accept a $k_p = 0$ or $k_c = 0$ case, as it is likely to assume that there would be an explicit requirement of installing a battery.

Fig. 8 shows the combinations of reduction of power and capacity of battery that leads to a set of yearly PV plant productions, limited by four lines: 100%, 97%, 95% and 80% of the maximum achievable production. The 100% curve expresses the limit of the region containing possible k_p and k_c combinations that lead to 100% PV plant production, which, therefore, should be seen as the set of combinations that minimise the size of the battery for 100% PV plant production.

Looking for battery design the so called C-rate (the ratio between P_{BAT} and C_{BAT}) of available batteries must be taken into account, so some lines that keep the C-rate relations have been added to Fig. 8. The intersections of previous lines and these C-rate lines, give information about the annual produced energy

[1] For interpretation of color in Fig. 5, the reader is referred to the web version of this article.

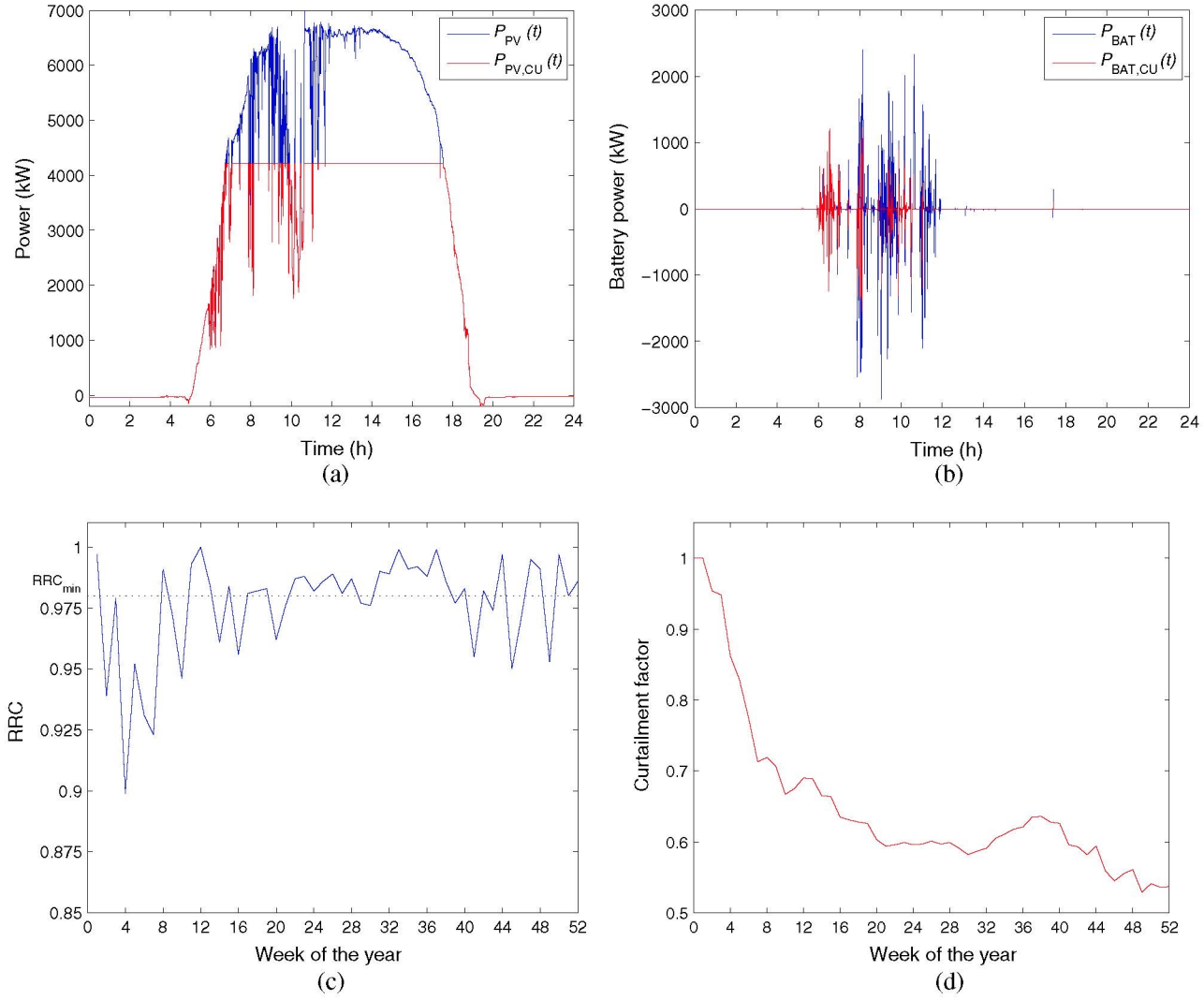

Fig. 5. Relation between curtailment and RR compliance, showing PV generation (a) and battery operation (b) during a day of week 31 of 2009 with reduced battery design power of $P_{BAT} = 0.1 \cdot P_{BAT,WF}$. Battery requirements for full RRC are lower for curtailed PV generation $P_{PV,CU}(t)$, than for the non-curtailed one $P_{PV}(t)$. Fluctuations are smaller due to curtailed $P_{PV,31} = 0.6 \cdot P_N$ (d) derived from bad RRC along the first weeks of the year (c), so battery operates less times.

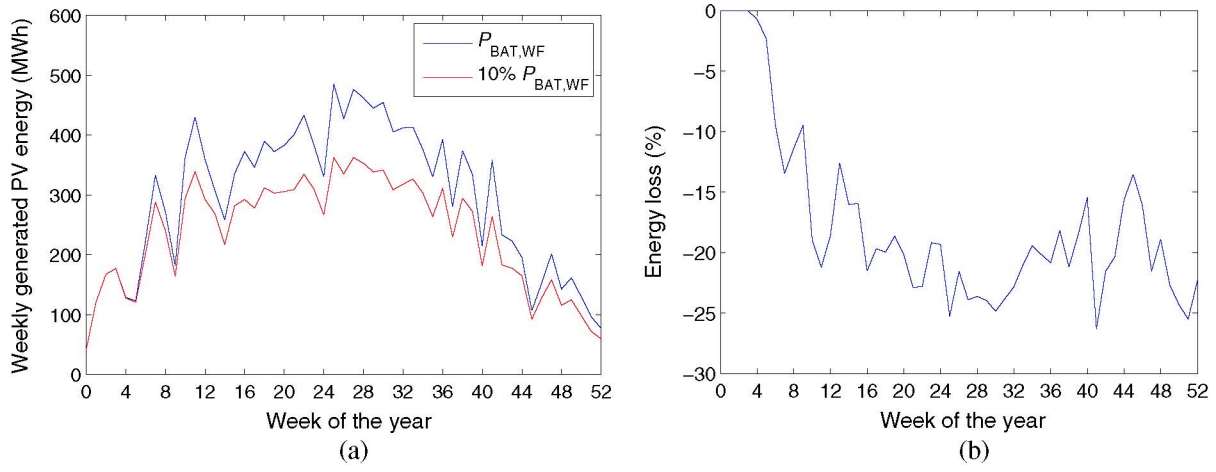

Fig. 6. (a) Weekly produced energy evolution for full power battery and 10% $P_{BAT,WF}$ battery. (b) Weekly energy loss with respect to full power battery, associated to the curtailment evolution caused by weekly *RRC*.

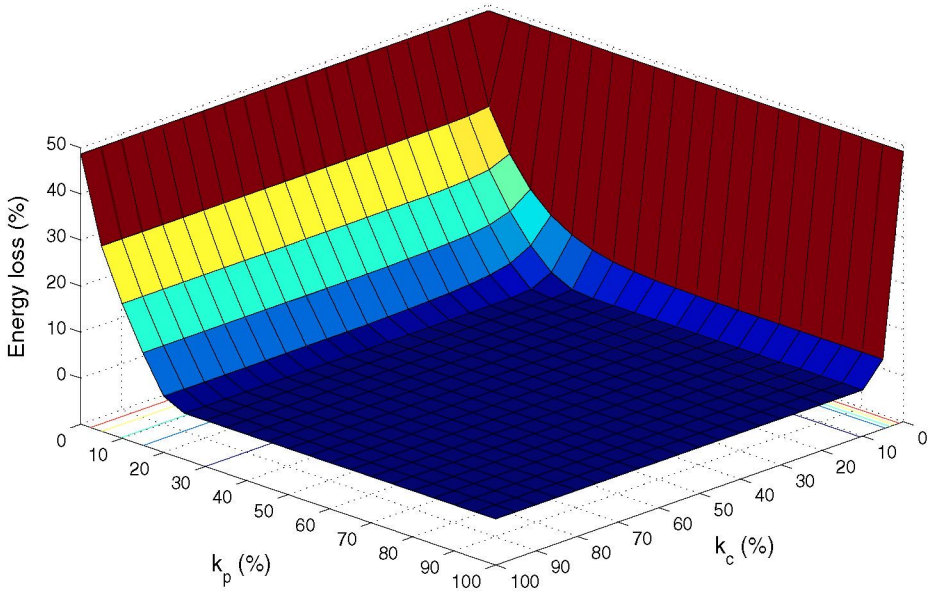

Fig. 7. Annual energy loss with respect to full sized battery case, in function of power and capacity reduction factors k_p and k_c.

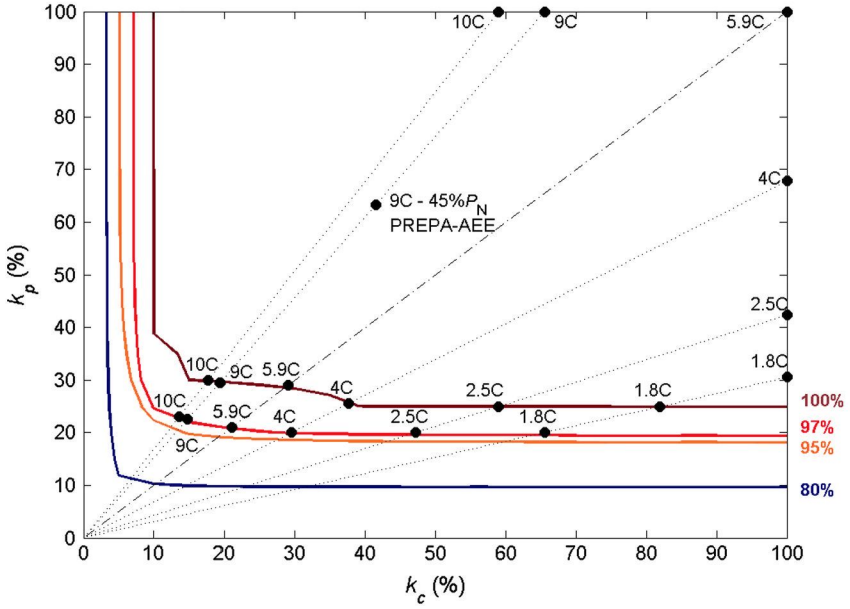

Fig. 8. Different annual production percentage limits with respect to maximum achievable one, depending on k_p and k_c combinations. Dotted lines represent k_p and k_c combinations that keep C-rates of commercial batteries, being them in reference to WF model battery C-rate (5.9C) dash-dot line. 9C is also included following PREPA-AEE minimum battery requirement.

using batteries with different C-rates available in the market (Saft, 2016; Samsung SDI, 2016) and for different gradual reductions of the battery power and capacity, showing the potential use of this study for designers of PV plants with batteries.

Two examples are going to be explained. On the one hand, the reduction of the battery rating 5.9C is going to be assessed, which corresponds to the one obtained as ideal for PV plant 100% RRC at its full size. As explained before, for a RR = 10%/min and $\Delta t = 2$ s, this battery is rated $P_{BAT,WF}$ = 5148 kW (71.1% P_N) and $2{\cdot}C_{BAT,WF}$ = 874 kWh (7.2 min). However, if the aim of the sizing is to achieve the 100% annual production reducing battery size to the maximum, k_p & k_c combination must be pointed on the cross between 5.9C-rate line and 100% production limit curve, resulting k_p = 0.29 and k_c = 0.29. This corresponds to P_{BAT} = 1493 kW (20.6% P_N) and C_{BAT} = 254 kWh (2.1 min).

On the other hand, a commercial 4C battery reduction is going to be assessed. The point which fulfils the maximum RRC according to the graph of Fig. 8 is rated P_{BAT} = 3493 kW (48.2% P_N) and C_{BAT} = 874 kWh (7.2 min). However, 100% annual production by reducing battery size to the maximum is achieved with k_p = 0.25 and k_c = 0.38, corresponding to P_{BAT} = 1313 kW (18.1% P_N) and C_{BAT} = 328 kWh (2.7 min).

Table 10 describes the most significant points of Fig. 8 corresponding with different C-rate batteries available in the market, regarding 100% and 97% annual PV generation targets. It can be seen that Fig. 8 and Table 10 are tools that open the door to project

Table 10
Battery size vs. PV energy production for different commercial C-rates. *C-rate for complying with PREPA-AEE proposed MTR of P_{BAT} = 45% P_N during 1 min and P_{BAT} = 30% P_N during 10 min.

E_{GRID} limit	C-rate	Power in kW (*% of* P_N)	Capacity in kWh (*min*)
100%	5.9	1493 (*20.6*)	254 (*2.1*)
	10	1544 (*21.3*)	155 (*1.3*)
	4	1313 (*18.1*)	328 (*2.7*)
	2.5	1287 (*17.8*)	515 (*4.3*)
	1.8	1287 (*17.8*)	715 (*5.9*)
	9*	1519 (*21.0*)	169 (*1.4*)
97%	5.9	1081 (*14.9*)	184 (*1.6*)
	10	1184 (*16.3*)	119 (*1.0*)
	4	1030 (*14.2*)	258 (*2.1*)
	2.5	1030 (*14.2*)	412 (*3.4*)
	1.8	1030 (*14.2*)	572 (*4.7*)
	9*	1158 (*16.0*)	129 (*1.1*)

designers for optimising the battery selection for the particular case of Puerto Rico, given the prices of different battery models available in the market.

Finally, it is worth mentioning a particular restriction recently proposed in Puerto Rico grid code by PREPA and the public utility AEE. There is an explicit requirement of installing a minimum ESS for both ramp rate control and frequency response. The system must be able to provide 45% of P_N during at least one minute for facing high power ramps, while it also must be able to provide 30% of P_N during ten minutes for frequency response. For the studied 7.2 MW PV plant, the required battery is rated P_{BAT} = 3260 kW (45% P_N) and C_{BAT} = 363 kWh (3 min), corresponding to a 9C relation, and comparing to the WF model size, it represents a reduction of k_p = 0.63 and k_c = 0.41, as shown in Fig. 8 and Table 10.

However, as long as the target is to keep the RR compliance above 98.5% along the year, the 45% of P_N requirement proposed by PREPA-AEE could be substituted by a lower requirement. As shown in the graph, 100% annual production is kept until a reduction of k_p = 0.3 and k_c = 0.19, corresponding to P_{BAT} = 1519 kW (21% P_N) and C_{BAT} = 169 kWh (1.4 min). That means that in terms of PV plant allowed energy production, the battery size minimum requirement could be further reduced down to this point without increasing penalties due to ramp rate failures. Nevertheless, note that this reduction could be detrimental to the frequency response service, so a simultaneous reduction analysis for this service should be carried out in future works.

The door for further research in this area is open and providing the statistics of radiation in different climatic zones, the application of this reduction analysis comparing energy production data series from multiple locations is an interesting work to be done.

4. Conclusions and outlook

This study has assessed a method for effectively reducing the size of the battery, in terms of power and energy capacity, below the design value given by the worst fluctuation model. It has been carried out addressing the impact of size reduction, analysing the sizing of practical batteries by taking into consideration, both, the fluctuation occurrence and the penalties in case of non-compliance of the prescribed ramp-rate limitations.

The simulations carried out for a 7.2 MW PV plant allow for deriving the relation between ramp rate compliance and battery size reduction. A model has been developed for describing the probability of occurrence of fluctuations that could not be absorbed by a certain reduced battery. The model accurately analyses the yearly ramp rate compliance and it shows that, given the low occurrence of fluctuations with high power or energy requirement, the battery can be considerably reduced from its size for full ramp rate compliance.

Moreover, the impact of the penalties caused by battery size reduction in the requirements particularly proposed in Puerto Rico grid codes has also been analysed. Taking into consideration weekly ramp rate compliance and the derived curtailments, the study has presented graphs that evaluate the produced energy with different combinations of battery power and capacity reductions according to different commercial C-rates.

In this case, for an optimal reduction of the worst fluctuation model battery sized $P_{BAT,WF}$ = 5148 kW (71.1% P_N) and $2{\cdot}C_{BAT,WF}$ = 874 kWh (7.2 min), 100% annual PV plant production is kept until P_{BAT} = 1493 kW (20.6% P_N) and C_{BAT} = 254 kWh (2.1 min). That means that for Puerto Rico particular case, the battery could be reduced to the 30% of the WF model size without losing PV generation. It is worth underlining that this battery reduction would not have a significant negative impact on the Puerto Rico system considering the low occurrence of the worst fluctuations.

Moreover, further size reduction feasibility could be assessed with the developed tools. It has been shown that using the results of the battery size reduction against the production decrease, it could be interesting to carry out further techno-economic analysis, evaluating the battery costs saving and the incomes losses caused by curtailed generated energy.

Acknowledgements

This work has been cofinanced by the European Commission in the frame of Seventh Framework Programme, in the context of PVCROPS project (PhotoVoltaic Cost reduction, Reliability, Operational performance, Prediction and Simulation), contract No. 308468.

References

CRE, 2012. Comisión Reguladora de Energía: Reglas generales de interconexión al sistema eléctrico nacional.
De la Parra, I., Marcos, J., García, M., Marroyo, L., 2016. Improvement of a control strategy for PV power ramp-rate limitation using the inverters : reduction of the associated energy losses. Sol. Energy.
De la Parra, I., Marcos, J., García, M., Marroyo, L., 2015. Control strategies to use the minimum energy storage requirement for PV power ramp-rate control. Sol. Energy 111, 332–343. http://dx.doi.org/10.1016/j.solener.2014.10.038.
Gallagher, K.G., Dees, D., Nelson, P., 2011. PHEV Battery Cost Assessment, DOE Vehicle Technologies Office Annual Merit Review. Washington D.C.
Gevorgian, V., Booth, S., 2013. Review of PREPA Technical Requirements for Interconnecting Wind and Solar Generation, NREL.
HECO, 2014. Hawaiian Electric Company: State of the System, Summary for ESS RFP.
Hoff, T.E., Perez, R., 2010. Quantifying PV power output variability. Sol. Energy 84, 1782–1793. http://dx.doi.org/10.1016/j.solener.2010.07.003.
Ina, N., Yanagawa, S., Kato, T., Suzuoki, Y., 2004. Smoothing of PV system output by tuning MPPT control. IEEJ Trans. Power Energy 124, 455–461.
Lave, M., Kleissl, J., 2013. Cloud speed impact on solar variability scaling – application to the wavelet variability model. Sol. Energy 91, 11–21. http://dx.doi.org/10.1016/j.solener.2013.01.023.
Lave, M., Kleissl, J., Arias-Castro, E., 2012. High-frequency irradiance fluctuations and geographic smoothing. Sol. Energy 86, 2190–2199. http://dx.doi.org/10.1016/j.solener.2011.06.031.
Marcos, J., de La Parra, I., García, M., Marroyo, L., 2014a. Control strategies to smooth short-term power fluctuations in large photovoltaic plants using battery storage systems. Energies 7, 6593–6619. http://dx.doi.org/10.3390/en7106593.
Marcos, J., Marroyo, L., Lorenzo, E., Alvira, D., Izco, E., 2011a. From irradiance to output power fluctuations: the PV plant as a low pass filter. Prog. Photovoltaics Res. Appl. 19, 505–510. http://dx.doi.org/10.1002/pip.1063.
Marcos, J., Marroyo, L., Lorenzo, E., Alvira, D., Izco, E., 2011b. Power output fluctuations in large scale PV plants: one year observations with one second resolution and a derived analytic model. Prog. Photovoltaics Res. Appl. 19, 218–227. http://dx.doi.org/10.1002/pip.1016.
Marcos, J., Marroyo, L., Lorenzo, E., García, M., 2012. Smoothing of PV power fluctuations by geographical dispersion. Prog. Photovoltaics Res. Appl. 20, 226–237. http://dx.doi.org/10.1002/pip.1127.
Marcos, J., Storkël, O., Marroyo, L., García, M., Lorenzo, E., 2014b. Storage requirements for PV power ramp-rate control. Sol. Energy 99, 28–35. http://dx.doi.org/10.1016/j.solener.2013.10.037.
Mazumdar, B.M., Saquib, M., Das, A.K., 2014. An empirical model for ramp analysis of utility-scale solar PV power. Sol. Energy 107, 44–49. http://dx.doi.org/10.1016/j.solener.2014.05.027.

Mills, A., Ahlstrom, M., Brower, M., Ellis, A., George, R., Hoff, T., Kroposki, B., Lenox, C., Miller, N., Stein, J., Wan, Y.H., 2009. Understanding Variability and Uncertainty of Photovoltaics for Integration with the Electric Power System. Lawrence Berkeley Natl. Lab.

Murata, A., Yamaguchi, H., Otani, K., 2009. A method of estimating the output fluctuation of many photovoltaic power generation systems dispersed in a wide area. Electr. Eng. Japan (English Transl. Denki Gakkai Ronbunshi) 166, 9–19. http://dx.doi.org/10.1002/eej.20723.

NERC, 2012. North American Electric Reliability Corporation: Interconnection Requirements for Variable Generation. Atlanta.

Perez, R., Hoff, T.E., 2013. Mitigating short-term PV output intermittency. In: 28th European Photovoltaic Solar Energy Conference and Exhibition. pp. 3719–3726.

PREPA, 2012. Puerto Rico Electric Power Authority Minimum Technical Requirements for Photovoltaic (PV) Generation Projects.

Saft, 2016. Energy Storage Systems Market Brochure. <www.saftbatteries.com>.

Samsung SDI, 2016. ESS for Utility Commercial. <www.samsungsdi.com>.

Tomson, T., Tamm, G., 2006. Short-term variability of solar radiation. Sol. Energy 80, 600–606. http://dx.doi.org/10.1016/j.solener.2005.03.009.

Van Haaren, R., Morjaria, M., Fthenakis, V., 2015. An energy storage algorithm for ramp rate control of utility scale PV (photovoltaics) plants. Energy 91, 894–902. http://dx.doi.org/10.1016/j.energy.2015.08.081.

Van Haaren, R., Morjaria, M., Fthenakis, V., 2014. Empirical assessment of short-term variability from utility-scale solar PV plants. Prog. Photovoltaics Res. Appl. 22, 548–559. http://dx.doi.org/10.1002/pip.2302.

Wood, D.L., Li, J., Daniel, C., 2015. Prospects for reducing the processing cost of lithium ion batteries. J. Power Sources 275, 234–242. http://dx.doi.org/10.1016/j.jpowsour.2014.11.019.

Woyte, A., Belmans, R., Nijs, J., 2007. Fluctuations in instantaneous clearness index: analysis and statistics. Sol. Energy 81, 195–206. http://dx.doi.org/10.1016/j.solener.2006.03.001.

Yoo, H.D., Markevich, E., Salitra, G., Sharon, D., Aurbach, D., 2014. On the challenge of developing advanced technologies for electrochemical energy storage and conversion. Mater. Today. http://dx.doi.org/10.1016/j.mattod.2014.02.014.